We are IntechOpen,
the world's leading publisher of
Open Access books
Built by scientists, for scientists

6,900
Open access books available

186,000
International authors and editors

200M
Downloads

Our authors are among the

154
Countries delivered to

TOP 1%
most cited scientists

12.2%
Contributors from top 500 universities

CLARIVATE ANALYTICS
BOOK CITATION INDEX
INDEXED

WEB OF SCIENCE™

Selection of our books indexed in the Book Citation Index
in Web of Science™ Core Collection (BKCI)

Interested in publishing with us?
Contact book.department@intechopen.com

Numbers displayed above are based on latest data collected.
For more information visit www.intechopen.com

Synergy Between Doppler Radar and Lidar for Atmospheric Boundary Layer Research

Chris G. Collier
National Centre for Atmospheric Science, University of Leeds
United Kingdom

1. Introduction

The principle of operation of radar and lidar is similar in that pulses of energy at wavelengths ranging from millimetres to metres for radar and 0.5 to 10 microns for lidar are transmitted into the atmosphere; the energy scattered back to the transceiver is collected and measured as a time-resolved signal. From the time delay between each outgoing transmitted pulse and the backscattered signal, the distance to the scatterer is inferred. The radial or line-of-sight velocity of the scatterers is determined from the Doppler frequency shift of the backscattered radiation. The systems use a heterodyne detection technique in which the return signal is mixed with a reference beam (i.e. local oscillator) of known frequency. A signal processing computer then determines the Doppler frequency shift from the spectra of the heterodyne signal. The energy content of the Doppler spectra can also be used to determine boundary layer eddy characteristics.

2. Characteristics of radar

The atmospheric boundary layer has been studied using weather radar extensively over the last forty years or so, such that networks of radars comprise systems sometimes operating unmanned in remote locations (see for example Atlas, 1990). Doppler radar operating at X, C or S-band (3cm, 5cm and 10cm wavelength respectively) has provided the opportunity to measure the reflectivity of target hydrometeors and the three dimensional wind structure of the lower parts of the atmosphere inferred from their motion (see for example Doviak and Zrnic, 1984). Typical parameters for a C-band radar are listed in Table 1. In addition, high power radar systems, such as the Oklahoma University Polarimetric radar for Innovations in Meteorology and Engineering (OU-PRIME) which operates at C-band and has a peak power of 1000 kW and a beamwidth of 0.45 degree (Palmer et al., 2011), provide information on the clear air structure of wind fields, and sometimes lower power systems may do the same at close range to the radar site. The detailed principle of operation has been described elsewhere in this book.

Millimetre-wave cloud radars exploit the fact that the echo intensity of Rayleigh scatterers increases with the inverse fourth power of the wavelength. These radars normally operate at 35 GHz and 94 GHz. UHF and VHF Doppler radar systems measure both wind speed and direction by detecting small irregularities in back scattered signals due to refractive index

inhomogeneities caused by turbulence. In the lower troposphere the refractive index inhomogeneities are mainly produced by humidity fluctuations. The clear air Doppler shift provides a direct measurement of the mean radial velocity along the radar beam. Typically a UHF wind profiler operates at 1290 MHz or 915 MHz with a peak power of 3.5 kW and a beamwidth of 8.5 degrees.

Wavelength / frequency	5 cm (C-band) / 5430-5800 MHz
Pulse repetition frequency	250-1200 Hz selectable
Bandwidth single PRF dual PRF	± 15.9 m s^{-1} ± 63.8 m s^{-1}
Sampling frequency - IF	60 MHz
Peak power	250 kW
Minimum Detectable Signal	-111 dBm
Beamwidth	1 degree
Down range resolution/ Maximum range	75 m 200 km
Transmitter type	Coaxial magnetron

Table 1. Typical parameters of a C-band radar (from Selex Gematronik)

Generally radars used for weather forecasting other than wind profilers have a resolution of about 100 m with an antenna having a diameter of about 4 m. Some research radars, such as the Chilbolton radar in the UK, provide measurements with a resolution at 100 km range using a 0.25 degree beamwidth (25 m diameter antenna) of 0.4 km. These resolutions certainly improve our understanding of the structure and behaviour of boundary layer phenomena, and examples will be described in this chapter. Nevertheless, boundary layer turbulent eddies may exist with characteristic length scales from tens of metres to fractions of a metre close to the ground. Such length scales require different instrumentation. Doppler lidar is an instrument providing high resolution, clear air measurements with resolutions of around 30 m, albeit over much shorter ranges than available from radar systems.

3. Characteristics of lidar

Lidar has been developed which operate in various atmospheric windows, namely the 10, 2, 1.5 and 1 micron spectral regions. Hardesty et al. (1992) compared the transmission, backscatter, refractive turbulence and Doppler estimation characteristics of a 2 and a 10 micron Doppler lidar system. Whilst backscatter at 2 microns in the free atmosphere is 4-10 times higher than for a 10 micron Doppler lidar, the effects of turbulence on the 2 micron system beyond a few kilometres range are significant, with the signal to noise ratio being reduced by about 6 dB at 5 km range. However, early equipment operated with CO_2 lasers at 10.6 micron wavelength, but involved delicate optical systems (Post and Cupp, 1990; Mayor et al., 1997; Pearson and Collier, 1999). The advent of fibre optic technology has enabled compact, robust equipment to be developed and operated remotely at wavelengths of 1.5 microns (Pearson et al., 2002, 2009). Table 2 shows the parameters of this type of Doppler lidar. The range resolution of 30 m is considerably smaller than that used in CO_2 lidars of about 112 m.

Wavelength	1.5 µm
Pulse repetition rate	20 kHz
Bandwidth	± 14 m s^{-1}
Sampling frequency	30 MHz
Points per range gate	6
Number of pulses averaged	20 000
Δr	18 m
Δp	30 m
Averaging time	1 s

Table 2. Parameters of 1.5 micron Doppler lidar. Range gate parameters: Δr relates to pulse length and Δp is the down range extent of the range gate used in the signal processing (from Pearson et al., 2009).

4. Advantages and disadvantages of radar and lidar

Both radars and lidars have advantages and disadvantages, and in this chapter a review of the accuracy with which measurements of boundary layer winds from both instruments is given. However both instruments offer complimentary information. Lidar backscatter is from widely dispersed aerosol particles in the clear air, but their concentration decreases away from the surface. Although thin clouds also provide backscatter, hydrometeors strongly attenuate the lidar signal. Radar backscatter is generally from hydrometeors, and therefore the operating range is much greater than that of lidar although this depends upon the wavelength used as short wavelength signals are attenuated.

Topography strongly controls the flux of momentum and energy between the terrain surface and the boundary layer. In-situ instruments have minimum spatial coverage, and radar cannot make measurements very close to the ground due to beam side lobes which produce ground clutter. With beamwidths of 0.1-1 m. rad., lidar transverse resolution is 20-200 times finer than the one degree (17.5 m. rad.) of weather radars (Drechsel et al., 2009). Lidar provides wide area coverage, although not as extensive as radar, but does not suffer from ground clutter problems. Hence lidar offers the opportunity to improve our knowledge of flow over complex terrain close to the ground surface (Barkwith and Collier, 2011). However radar can provide detailed information in the boundary layer over very wide areas, particularly related to the development of convective systems.

5. Wind profiling

5.1 Single instrument measurements

Measurements of the vertical profile of wind may be made using Doppler lidar and both weather radars and UHF / VHF profilers. There are two modes that can be utilised for this. The beam can be scanned in a cone at fixed elevation and the resulting data fitted to a sine wave. This is known as the velocity-azimuth display (VAD) approach as described by Browning and Wexler (1968). This has been the preferred technique for radar systems although it has also been used with lidar systems. An alternative approach uses three fixed line of sights from which a vector analysis provides the three components of the wind (u, v and w) as described by Werner (2005).

Using the VAD technique Bozier et al. (2004) compared the average horizontal wind velocity difference and average standard deviation between a CO_2 Doppler lidar and tethered balloon borne turbulence probe measurements at a site in Eastern England as shown in Table 3. The in situ sensor captures a higher frequency turbulence component in the wind velocity data due to the higher measurement rate, 4 Hz, compared to the lidar data sampling rate of 0.1 Hz.

Measurement run	Height range (m)	Wind velocity difference (m s^{-1})	Lidar standard deviation (m s^{-1})	Balloon standard deviation (m s^{-1})
L1, B1	350–750	0.53	1.04	0.80
L2, B2	180–530	0.38	1.50	0.78
L3, B3	210–530	0.34	1.39	1.14
L4, B4	350–900	0.19	1.28	0.67

Table 3. Comparison of lidar and balloon borne instrument probe derived horizontal wind profiles (from Bozier et al., 2004)

Pearson et al. (2009) suggests that the three-beam technique may offer a better option in regions where the flow is not constant and laminar over the disc swept out by the VAD scan for example where topography influences the flow field. They showed examples of both approaches in a study of the performance of a 1.5 micron Doppler lidar. Based on 51 days continuous, unattended operation at a site in southern England, Figure 1 shows the results of an inter-comparison carried out on 13 September 2007 between a UHF radar and lidar data. There is no cloud cover. The wind speed data are less well correlated possibly due to ground clutter contamination of the radar velocity data, or a reduction in the Signal-to-Noise (SNR) leading to a larger degree of uncertainty in the sine-wave fit procedure. Similar results have been found using a 10.6 micron CO_2 Doppler lidar by Mayor et al. (1997), who compared vertical velocities derived from a 915 MHz radar profiler. A difference between the two instruments of -0.81 cm s^{-1} was found. It was noted that the difference may be due to the different sizes of the sampling volumes, the spatial separation of the two measurements and the different SNRs. Comparisons of VAD winds derived from Doppler lidar reported by Drechsel et al. (2009) deviated from wind profiler measurements by less than 1.0 m sec^{-1} and -1 degree, and only 0.1 m sec^{-1} and 2 degrees from radiosonde data.

5.2 Dual-doppler systems

A single Doppler radar or lidar measures the field of wind velocities that are directed towards or away from the instrument. Doviak and Zrnic (1984) describe how a second Doppler radar spaced far from the first produces a field of different radial velocities which can be vectorially synthesized to retrieve the two dimensional velocities in the plane containing the radials.
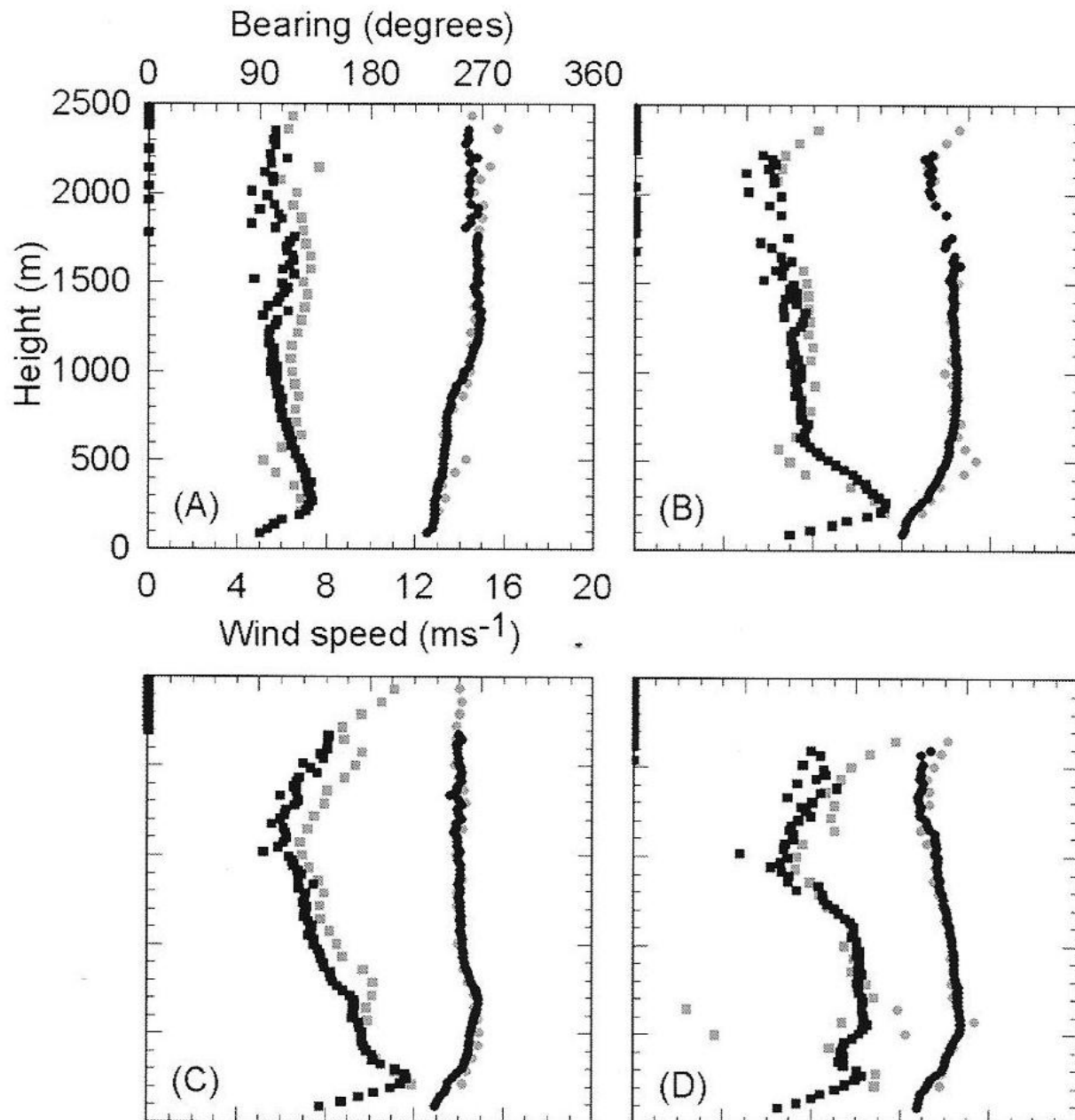
Fig. 1. Radar and lidar profiles from the evening of 13 Sept. 2007. The lidar scan took 9 min and the radar data are for a 10-min average. (A)-(D) Start times of 1900, 2100, 2200 and 2300 UTC respectively. The circles and squares show the bearing and speed data respectively (grey radar and black lidar) (from Pearson et al., 2009)

This is greatly simplified if this operation is performed in cylindrical coordinates with axis chosen to be in the line connecting the two radars 1 and 2, referred to as the baseline. The mean Doppler velocity is corrected for the reflectivity-weighted mean terminal velocity of the scatterers w_t . Hence the estimate of the radial component of air motion is:

$$v_{1,2} = v_{1,2}' + \overline{w_t} \sin \Theta_{e1,2}$$

where $v_{1,2}'$ are the mean Doppler target velocities measured by radars 1,2 at data points and w_t is positive. To estimate w_t an empirical expression such as that given by Atlas et al. (1973) can be used. The estimated radial velocities $v_{1,2}$ of the air can be interpolated to uniformly spaced grid points in planes at an angle α to the horizontal surface containing the baseline. The wind component w_α normal to the plane is obtained by solving the continuity equation in cylindrical coordinates:

$$1/r \, \partial/\partial r \, (r\rho w_r) + 1/r \, \partial/\partial x \, (\rho w_\alpha) + \partial/\partial s \, (\rho w_s) = 0$$

with the boundary condition w = 0 at the ground. Generally this approach covers a smaller area compared to the full dual-Doppler coverage and may contain residual errors.

An improved albeit similar approach has been developed by Bousquet and Chong (1998) for three dimensional wind retrieval from multiple airborne Doppler radars, called the Multiple Doppler Synthesis and Continuity Adjustment Technique (MUSCAT). It was extended for application over both flat or complex terrain by Chong and Cosma (2000), and for ground-based radar systems by Chong and Bousquet (2001). An alternative computationally inexpensive plane-to-plane solution known as the Multiple Analytical Doppler (MANDOP) system has been described by Tabary and Scialom (2001).

In 2003 two mobile Doppler lidars were sited at either end of a disused runway approximately 1.6 km apart at RAF Northolt in West London (Collier et al., 2005). The aim was to investigate the optimal lidar configuration to measure wind flow turbulence characteristics. Three dual-lidar configurations are shown in Figure 2. Figures 2a and 2c show data taken with the two lidars where the beams cross at a point, which is in the vertical plane defined by the line joining the two lidar positions. With each lidar system the radial velocities along the beams were measured every five seconds. The two radar computer clocks were first synchronised, and then for the different configurations, the time series of data were taken. Table 4 gives statistics derived from operating the lidar systems as in configuration 2c. The data were taken for a period of 700 seconds, and for different heights over a period of approximately 50 minutes. The errors in the vertical velocities from this dual-Doppler lidar deployment were analysed by Davies et al. (2005). It was found that the spread in vertical velocities due to the combined effects from instrumental errors of the two lidars can in some cases act to cancel each other out, although on other occasions this was not the case. We discuss the implications of this in the next section.

Drechsel et al. (2009) applied the MUSCAT processing system to dual-Doppler lidar data collected during the Terrain – induced Experiment (T-REX) in the spring of 2006. The flow pattern derived from 19 three dimensional wind fields revealed differences of wind speed and direction of less than 1.1 m sec^{-1} and 3 degrees on average compared to radiosonde and wind profiler data. The average vertical motion from MUSCAT was -0.24 m sec^{-1} compared to -0.52 m sec^{-1} from wind profiler data and -0.32 m sec^{-1} from radiosonde data.

Height (m)	Mean horizontal wind in direction of the lidar axis (m/s)	Mean vertical Wind (m/s)	Std. dev. of wind in direction of the lidar axis (m/s)	Std. Dev. of vertical wind (m/s)
100	-0.05	1.1	0.50	3.43
200	1.52	-0.90	0.59	1.45
400	0.77	-0.66	0.59	1.78
709	0.68	-0.83	1.49	1.13

Table 4. Means and standard deviations of the horizontal and vertical winds. The horizontal wind is the wind in the direction of the axis joining the two lidars. The heights of the data are determined by the crossing points of the two lidar beams as shown in the configuration of Figure 2c. The lidar data were taken from 1134-1224 UTC 23 July 2003 (from Collier et al. (2005)

(a)   (b)

c
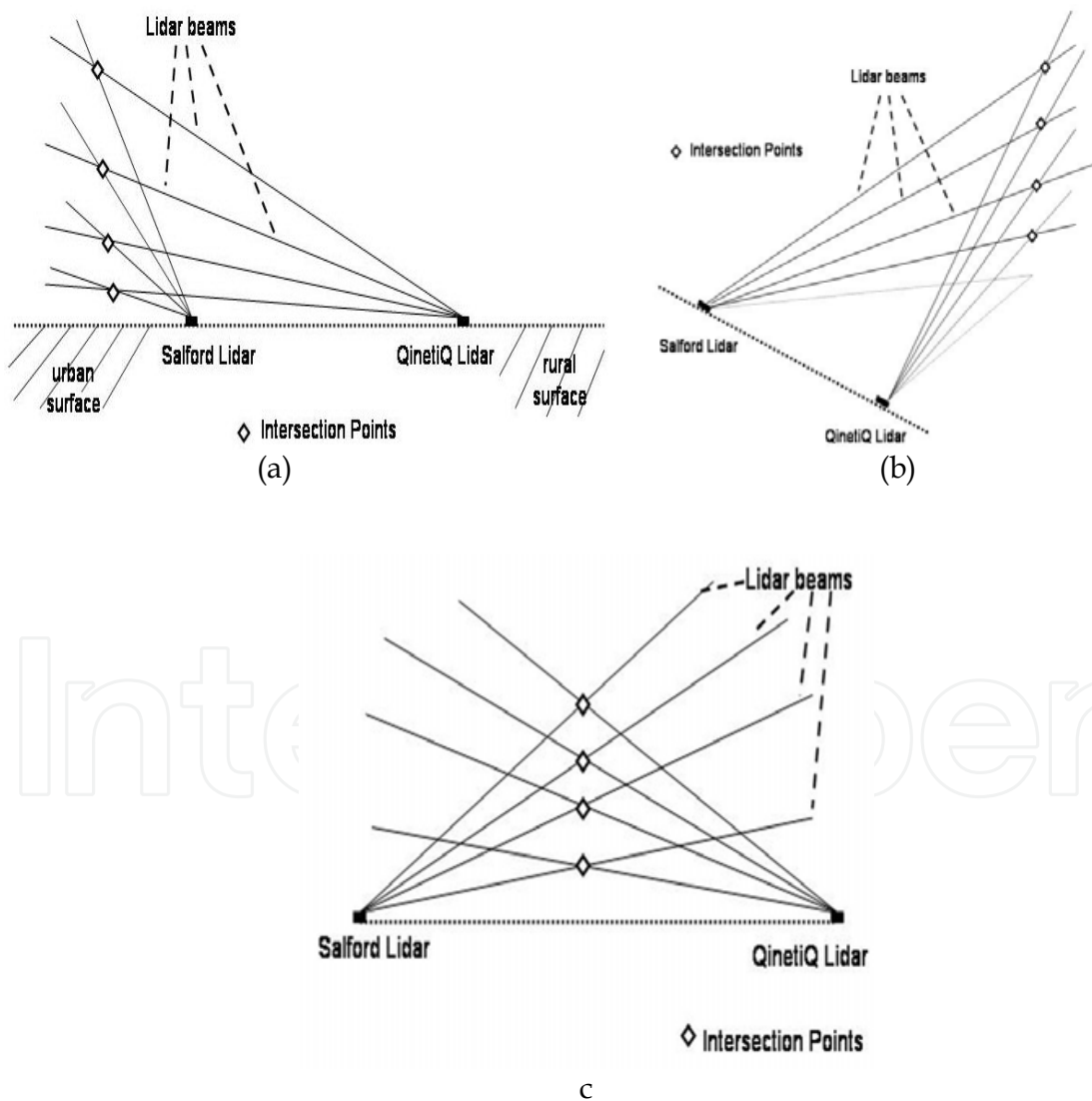
Fig. 2. Dual-lidar configurations. Diamonds denote beam intersection points (from Collier et al., 2005)

6. Measuring turbulent structure

A comprehensive review of the use of radar to measure the morphology of the boundary layer is provided by Gossard (1990), who also provides a review of the use of Doppler radar to measure turbulent velocity variance and covariance. VAD scans do not produce perfect sinusoids, and their derived time series are perturbed by random turbulent fluctuations at scales larger than the radar pulse volume, but much smaller than the diameter of the VAD. Wilson (1970) and Wilson and Miller (1972) developed a procedure for extracting quantitatively the variances and covariances of u, v and w. This was developed further by Kropfli (1984) who measured profiles of vertical momentum flux through the convective boundary layer as shown in Figure 3.
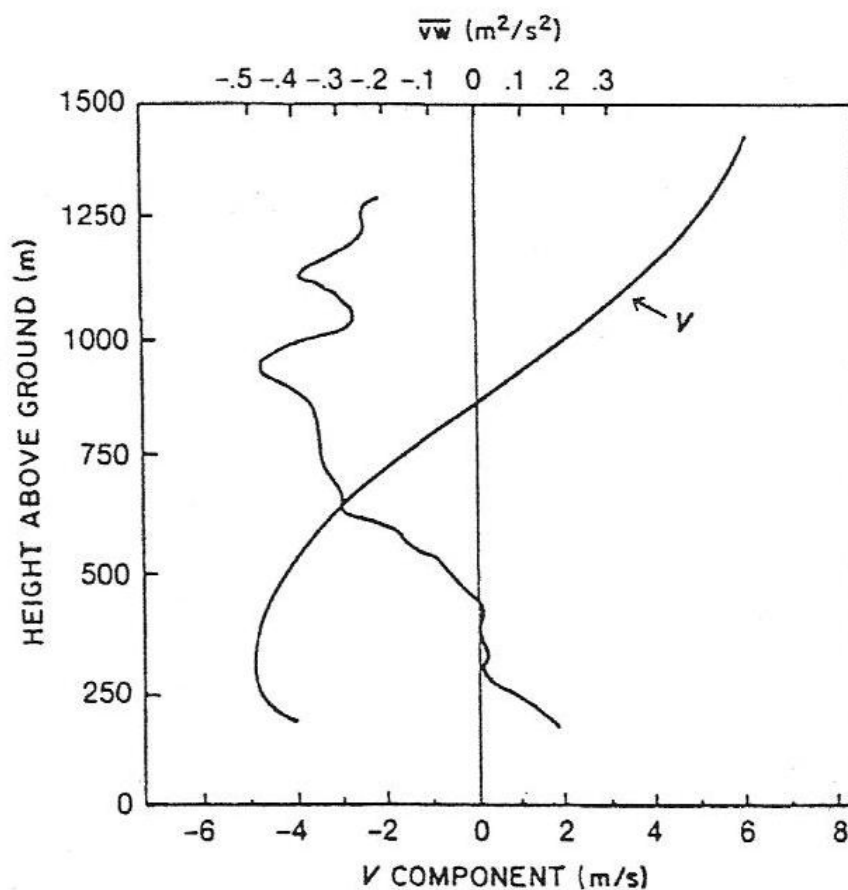
Fig. 3. Single radar measurement of vertical profile of momentum flux through the boundary layer by the method of Wilson (1970). Data are from a 100-min period beginning at 12-3 MDT during the PHOENIX experiment (from Kropfli, 1984)

The radar Doppler spectral width has also been used to extract small-scale turbulence information from spectral broadening due to wind shear, the radar antenna properties and the variance of the velocity component in the radial direction due to turbulence. In particular, the eddy dissipation rate can be measured, the first attempt to do this being by Gorelik and Mel'nichuk (1963). Table 5 is a summary of the literature on the measurement of turbulent energy dissipation (ε). Note that both radar and lidar have been used to measure this quantity.

Type	Typical Values of ε x 10³ (m² sec⁻³)	Typical estimate	Reference
D_N	0.2	Model	Simmons and Hoskins, (1978)
D_{GW}	6 (Over major mountains)	Model	Shutts (2005)
D_C	1-10	Radar and aircraft observations	Meischner et al (2001)
D_F	1000 (within the surface layer) 2 (in shallow sloping frontal layers); 3 (close to the ground before surface front passes); 20 (jet stream level; clear air turbulence) 30 (jet stream level; clear air turbulence)	Hot-wire anemometer at 3m Radar observations Aircraft observations Radar observations	Piper and Lundquist (2004) Chapman and Browning (2001); Chapman and Browning (2001); Kennedy and Shapiro (1975, 1980) Gage et al (1980)
D_B (Urban areas)	Up to 4 (urban areas) 0.2 – 6.2 (urban areas)	Lidar observations at several hundred metres Lidar observations	Davies et al (2004); Davis et al (2008)

Table 5. Energy dissipation rates, ε (m² sec⁻³) (from Collier and Davies, 2009)

Generally the vertical velocity in the turbulent boundary layer is very small, and difficult to measure. It is clear that significant temporal averaging is necessary. Kropfli (1984) suggested averaging over 20 minutes for VAD radar data, whereas Davies et al. (2005) averaged lidar data over 10 to about 50 minutes. However, the errors in the wind velocity, particularly those in w were thought by Sathe et al. (2011) to prelude the use of Doppler lidar with the VAD technique from measuring boundary layer turbulence precisely. This conclusion is not necessarily appropriate when two lidars are used as demonstrated by Davies et al. (2005) and Pearson et al. (2009).

In order to investigate the detailed structure of the turbulent motion above the Urban Canopy Layer (UCL), Davies et al. (2004) compared Doppler lidar-measured turbulent structure functions with those derived using the Von Karman model of isotopic turbulence in the inertial sub-range. Making allowance for the spatial averaging of the lidar pulse volume, the correspondence is comforting (Fig. 4). Hence, estimates of the integral length-scale, the dominant spatial scale of the turbulence above the UCL, can be made from the fit of the model to the observations, giving a range from 250–400 m. In addition, measurements were made of the velocity covariance power spectra, and the corresponding eddy dissipation rates are shown in Fig. 5. The slope of the spectra within the inertial sublayer is usually −5/3, although this depends upon the presence of inversion layers and the strength of the turbulence. The fact that the spectrum falls off faster than −5/3 may indicate that the turbulence approaches isotropy locally in the inertial range (Lumley, 1965). However, in the

case of the lidar measurements the fall off at less negative wave numbers is more likely to be due to the spatial averaging of the data over the beam. Climatologies of urban and rural eddy dissipation rates are needed to evaluate the urban effects.
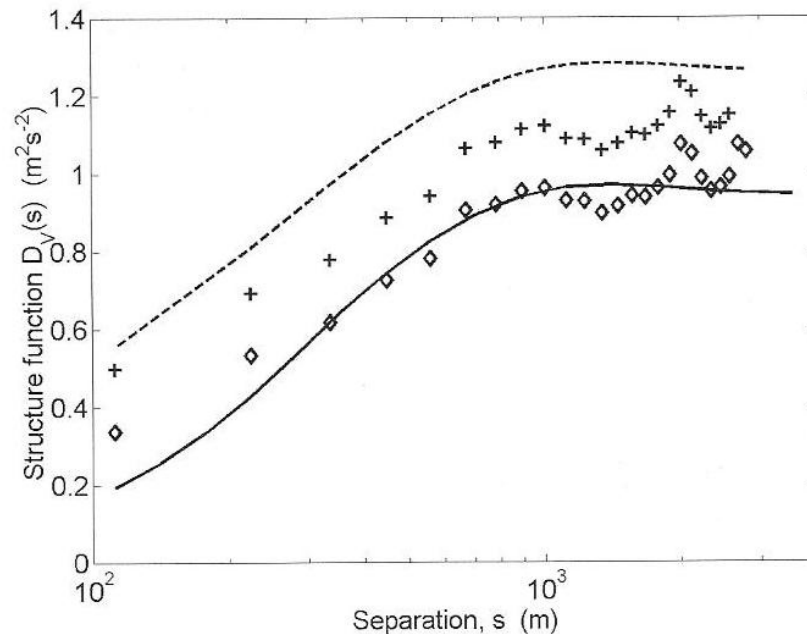

Fig. 4. Comparison of lidar measurements of structure function with the Von Karman model over Salford, Greater Manchester at 1317 UTC 2 May 2002. The upper dashed line represents the uncorrected model and the lower thick line the corrected model; crosses are uncorrected lidar measurements and diamonds are the corrected lidar measurements. (From Davies et al. 2004.)
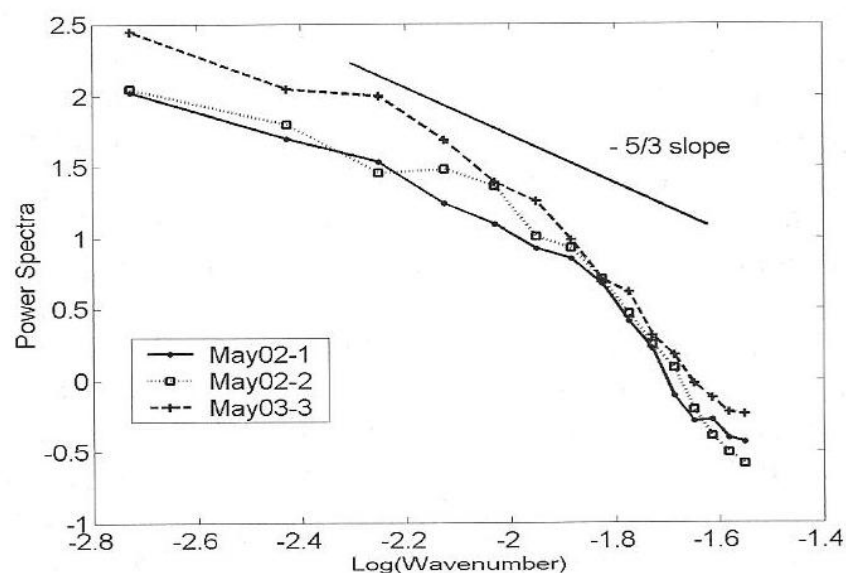
Fig. 5. Covariance power spectra and eddy dissipation rates, ε, over Salford, Greater Manchester, derived from line-of-sight measurements made during the SALFEX experiment for three datasets as indicated. The values of ε for the three curves range from 1.1 to 4.3 × 10^{-3} m^{2}sec^{-3}. (From Davies et al. 2004.)

Recently Krishnamurthy et al. (2011) reported Doppler lidar measurements of turbulent kinetic energy dissipation rate, integral length scale and velocity variance assuming a theoretical model of isotropic wind fields during the T-REX Project. Corrections to address the complications inherent in volumetric averaging of radial velocity over each range gate, noise in the data and the assumption made regarding the effects of smaller scales of motion were considered and tested. Comparisons between the lidar and tower measurements supported the soundness of the lidar measurements of boundary layer turbulence.

7. Doppler radar and lidar measurements of boundary layer phenomena

7.1 Storm outflows

One of the most difficult forecasting problems remains the identification of when and where convective cells develop. Two facets of this problem are (a) how first-generation convective cells are triggered in an environment which has been previously quiescent for a period, but which becomes more and more unstable; and (b) for convective cells that persist, how and where subsequent generations of cells are triggered by the propagation of cold outflows from existing cells. Over the years there have been many studies addressing these issues using radar data (see for example Bader et al., 1995). Indeed, it is well known that first generation convective cells may be triggered by orographic uplift, and by land surface heterogeneity caused by variations in the temperature and moisture fields.

Collier and Davies (2004) describe a study of the pre-storm environment for a case study using a Doppler lidar located at Northolt, North West London, a C-band weather radar sited at Chenies north of London and the S-band Chilbolton radar. It was noted that the Doppler lidar and the weather radar data complement each other. Figure 6 shows Chenies and Chilbolton radar images, a PPI from the Doppler lidar and a LDR PPI from the Chilbolton radar. An outflow boundary is evident in all the images. A reversal of the wind direction at low levels is shown near the lidar site. The Chenies radar shows a thin line of broken echoes about 12 km to the north and north west of the main area of convective rain. The Chilbolton radar Linear Depolarisation Ratio (LDR) suggests that the radar targets in the outflow region are probably not raindrops, but may be particulate matter (straw, dust). The Doppler radial velocities observed by Chilbolton are consistent with the lidar measurements in the figure.

Similar measurements of an outflow have been reported by Collier et al. (2008). This study illustrates the difficulty of measuring an outflow using a radar, in this case the DLR C-band radar. In Figure 7a an outflow from a thunderstorm over the Rhine Valley is partially observed by the radar, but the details are not clear as there is some confusion with ground clutter. Figure 7b shows Doppler lidar measurements of the vertical velocities made from Achern in the Rhine Valley. Here the outflow is clear. It is about 800 m deep, and a cap cloud is observed near the leading edge. The peak kinetic energy dissipation rate was calculated to be 0.18 $m^2 sec^{-3}$.

7.2 Observing smoke plumes

Combined observations of smoke plumes using lidar and radar have not been extensively reported. Such plumes may be generated from wild fires, or from prescribed (planned) burns. The plumes may contain lofted debri as the primary source of targets, although smoke and condensed water droplets may also be evident. Banta et al. (1992) used Doppler radar and

lidar to observe both prescribed and wild fires. Figure 8 shows Doppler lidar measurements of plumes over Helsinki produced from forest fires in North West Russia. The correlation between the lidar backscatter data and the retrieved vertical velocities shows convective updrafts containing the particulate-laden air from the cleaner air contained in downdrafts.
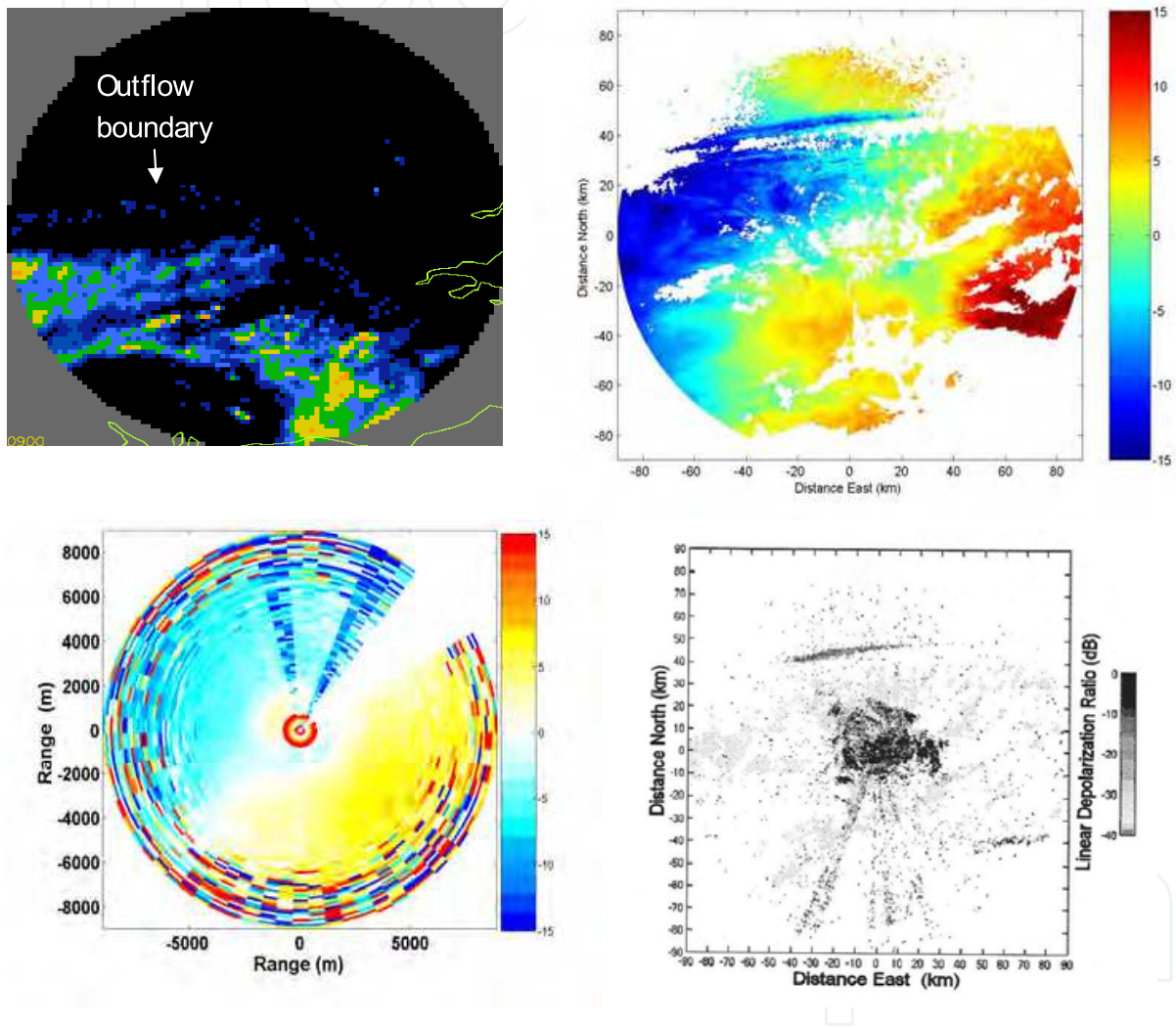

Fig. 6. (a) (top left) Chenies radar images on 16 July 2003 [Blue less than 1 mm h^{-1}; yellow 2-4 mm h^{-1}; grid 2 km x 2 km maximum range 75 km]; (b) (top right) Chilbolton unfolded radial velocities 16 July 0903 UTC in m sec^{-1} [negative away from the radar]; (c) (bottom left) Doppler lidar PPI [10 deg.] radial velocities [m sec^{-1}] 16 July 2003.0850 UTC [negative towards the lidar]. Note the wind reversal at low levels; (d) (bottom right) Chilbolton radar Linear Depolarisation Ratio (LDR) 16 July 0903 UTC (from Collier and Davies, 2004).
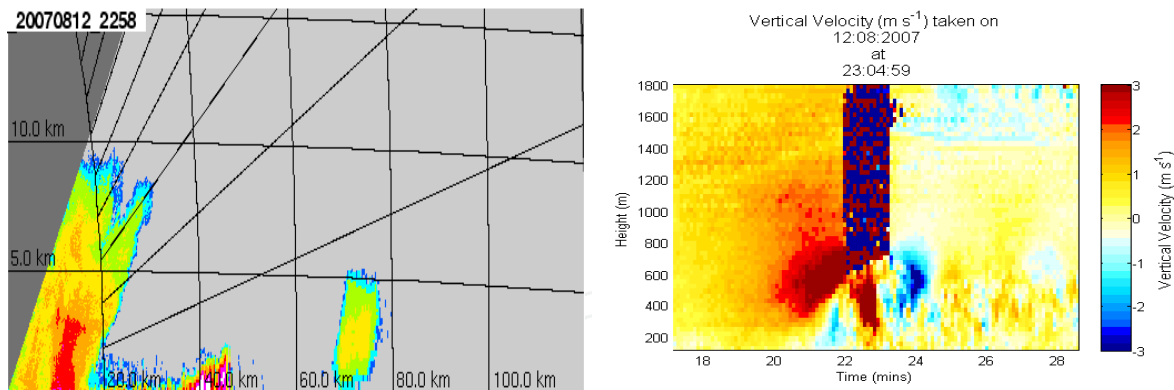
Fig. 7. Illustrating (a) RHI from the DLR Poldirad radar located at Waltenheim-sur-zorn towards the Supersites Achern (36 km), Hornisgrinde (46 km) and AMF (62 km) at 22.58 UTC 12 August 2007; and (b) vertical velocity measured at 23.04 UTC by Doppler lidar located at Achern on 12 August 2007 (from Collier et al., 2008).
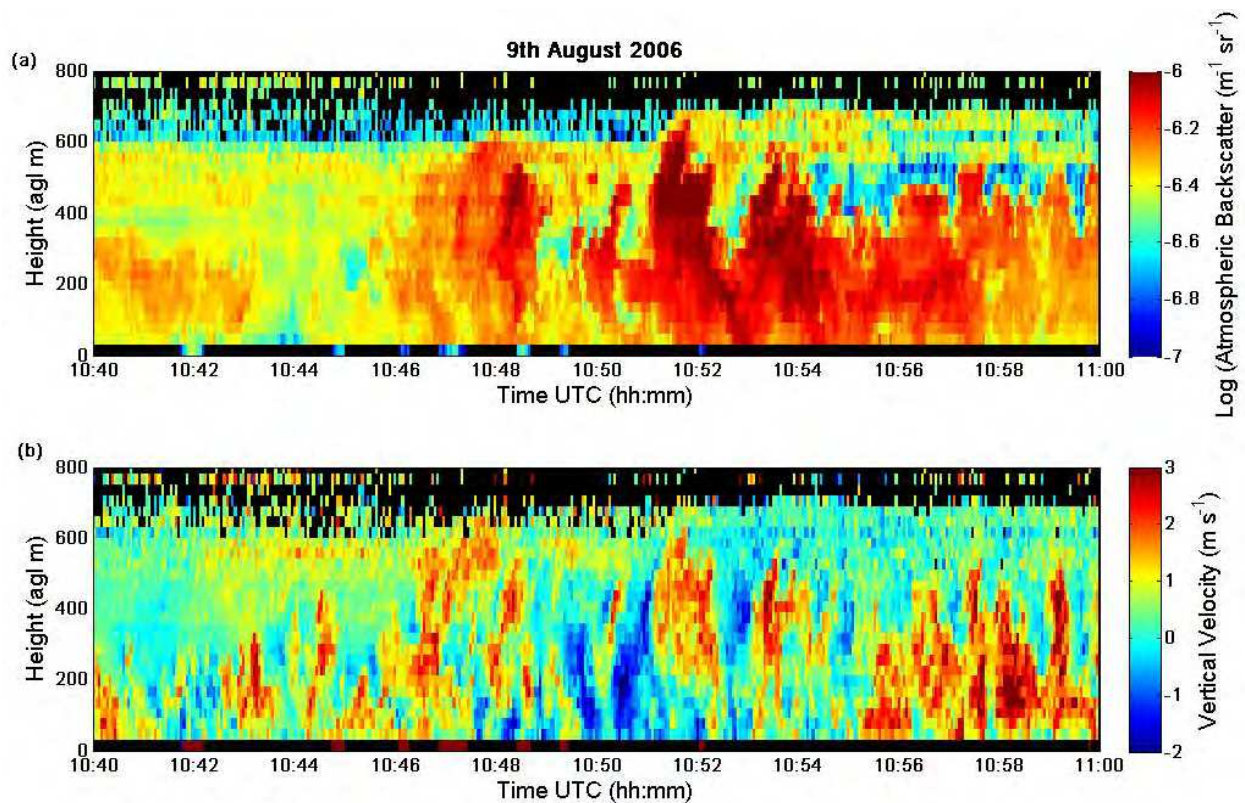

Fig. 8. Time series of lidar atmospheric backscatter and vertical velocity measurements taken on 9 August 2006 1040-1100 UTC in Helsinki, Finland. The log of the atmospheric backscatter is shown in (a) with the vertical velocity data from the lidar shown in (b). The vertical axis shows height above ground level (m) and the horizontal axis is time (UTC) (from Bozier et al., 2007).

7.3 Understanding convection

Skewness is a measure of asymmetry in the distribution of vertical velocity perturbations. Positive skewness at the surface suggests narrow intense updrafts from the surface and broad downdrafts (fair weather, clear). Negative skewness suggests sharp, narrow downdrafts and larger areas of weaker updraft, rather like "upside down" surface heating driven by turbulence on a cloudy day. Skewness may be calculated using,

$$S = w'^3 / (w'^2)^{3/2}$$

Bother Doppler radar and Doppler lidar are capable of measuring vertical velocity and they can measure skewness throughout the boundary layer. Knowing the skewness can help understand the structure of convection (see for example Hogan et al., 2009).

Although weather radars are available around the edges of tropical rain forests, there have as yet been only a few studies combining radar wind profilers and lidar (ceilometers) data (Grimsdell and Angevine, 1998). Vila-Guerau de Arellano et al. (2009) studied the isoprene fluxes in the tropical rain forest environment, but recommended the continued use of a radar wind profiler or Doppler lidar. Pearson et al. (2010) used a Doppler lidar to measure the diurnal cycle of the wind field in the tropical boundary layer, Sabah, Borneo.

8. Concluding remarks

Since radar and lidar provide measurements of backscatter and atmospheric motion based upon different targets, it is clear that much useful complementary information on atmospheric phenomena and processes can be obtained. Used together these instruments provide a powerful mechanism by which to enhance our knowledge of the atmosphere and develop improved forecasting procedures of a wide range of phenomena. Both technologies offer instrumentation capable of continuous unattended operation.

9. References

Atlas, D. (ED) (1990) *Radar in Meteorology*, Am. Met. Soc., 806pp

Atlas, D., Srivastava, R.C. and Sekhon, A.S. (1973). Doppler radar characteristics of precipitation at vertical incidence, *Rev. Geophys. Space Phys.*, 2, pp 1-35

Bader, M.J., Forbes, G.S., Grant, J.R., Lilley, R.B.E. and Waters, A.J. (1995). *Images in Weather Forecasting. A practical guide for interpreting satellite and radar imagery*, Cambridge University Press, 499pp

Banta, R.M., Olivier, L.D., Holloway, E.T., Kropfli, R.A., Bartram, B.W., Cupp, R.E. and Post, M.J. (1992). Smoke-column observations from two forest fires using Doppler lidar and Doppler radar, *J. Appl. Met.*, 31, 1328-1349

Barkwith, A. and Collier, C.G. (2011). Lidar observations of flow variability over complex terrain, *Meteor. Appl.*, 18, 372-382

Bousquet, O. and Chong, M. (1998). A Multiple-Doppler Synthesis and Continuity Adjustment Technique (MUSCAT) to recover wind components from Doppler radar measurements, *J. Atmos. Ocean. Tech.*, 15, pp 343-359

Bozier, K.E., Pearson, G.N. and Collier, C.G. (2007). Doppler lidar observations of Russian forest fire plumes over Helsinki, *Weather*, 62, no 8, pp 203-208

Browning, K.A. and Wexler, R. (1968). The determination of kinematic properties of a wind field using Doppler radar, *J. Appl. Met.*, 7, pp 105-113

Chong, M. and Cosma, S. (2000). A formulation of the continuity equation of MUSCAT for either flat or complex terrain, *J. Atmos. Ocean. Tech.*, 17, pp 1556-1565

Chapman, D. and Browning, K.A. (2001). Measurements of dissipation rate in frontal zones, *Quart. J. R. Met. Soc.*, 127, pp 1939-1959

Collier, C.G. and Davies, F. (2004). Observations of the development of the convective boundary layer using radar and Doppler lidar, *Proc. European Radar Conf. (ERAD)*, Copernicus GmbH, Visby, Gotland, Sweden, 6-10 Sept. 2004, ISBN 3-936586-29-2

Collier, C.G. and Davies, F. (2009). "Representing energy drain in Numerical Weather Prediction models induced by boundary layer sub-grid scale processes", *Atmos. Sci. Letters,* 10, Issue 3, DOI: 10.1002/asl.222, 146-151

Collier, C.G., Davies, F., Bozier, K.E., Holt, A., Middleton, D.R., Pearson, G.N., Siemen, S., Willetts, D.V., Upton, G.J.G. and Young, R.I. (2005). Dual Doppler lidar measurements for improving dispersion models, *Bull. Am. Met. Soc.*, 86, pp 825-838

Collier, C.G., Davies, F., Davis J.C., Pearson, G.N. and Hagen, M. (2008). Doppler radar and lidar observations of a thunderstorm outflow, *Proc. 5th European Conf. on Radar Met. and Hydrology (ERAD),* Copernicus GmbH, June, Helsinki, ISSN 978-951-697-676-4

Davies, F., Collier, C.G., Pearson, G.N. and Bozier, K.E. (2004). Doppler lidar measurements of turbulent structure function over an urban area, *J. Atmos. Ocean. Tech.*, 21, pp 753-761

Davies, F., Collier, C.G. and Bozier, K.E. (2005). Errors associated with dual Doppler-lidar turbulence measurements, *J. Opt. A: Pure Appl. Opt.*, 7, pp S280-S289

Davis, J.C. Collier, C.G., Davies, F. and Bozier, K.E. (2008). Spatial variations of sensible heat flux over an urban area measured using Doppler lidar, *Meteor. Appl.*, 15, pp 367-380

Doviak, R.J. and Zrnic, D.S. (1984). *Doppler Radar and Weather Observations*, 2nd Ed., Academic Press, 562pp

Drechsel, S., Chong, M., Mayr, G.J., Weissmann, M., Calhoun, R. and Dornbrack, A. (2009). Three-dimensional wind retrieval: application of MUSCAT to dual-Doppler lidar, *J. Atmos. Ocean. Tech.*, 26, pp 635-646

Gage, K.S., Green, J.L. and Van Zandt, T.E. (1980). Use of a Doppler radar for the measurement of atmospheric turbulence parameters from the intensity of clear-air echoes, *Radio Sci.*, 15, pp 407-416

Gorelik, A.G. and Mel'nichuk, Yu.V. (1963). Radar study of dynamic process in the atmosphere, Tr. Vses. Nov. Meteor. Souesh. No5

Gossard, E.E. (1990). Radar research on the atmospheric boundary layer, in *Radar in Meteorology*, ed. D. Atlas, Am. Met. Soc., Boston, pp 477-527

Grimsdell, R.W. and Angevine, W.M. (1998). Covective boundary layer height measurement with wind profilers and comparison to cloud base, *J. Atmos. Ocean. Tech.*, 15, pp 1331-1338

Hardesty, R.M., Grund, C.J., Post, M.J., Rye, B.J. and Pearson, G.N. (1992). Measurements of winds and cloud characteristics: a comparison of Doppler lidar systems, Int. *Geoscience & Remote Sensing (Houston, IX, 1992)* Session TA-P, Paper 2

Hogan, R.J., Grant, A.L.M., Illingworth, A.J., Pearson, G.N. and O'Connor, E.J. (2009). Vertical velocity variance and skewness in clear and cloud-topped boundary layers as revealed by Doppler lidar, *Quart. J. R. Met. Soc.*, 135, pp 635-643

Kennedy, P.J. and Shapiro, M.A. (1975). The energy budget in a clear air turbulence zone as observed by aircraft, *Mon. Wea. Rev.*, 103, pp 650-654

Kennedy, P.J. and Shapiro, M.A. (1980). Further encounters with clear air turbulence in research aircraft, *J. Atmos. Sci.*, 37, pp 986-993

Krishnamurthy, A., Calhoun, R., Billings, B. and Doyle, J. (2011). Wind turbulence estimates in a valley by coherent Doppler lidar, *Meteor. Appl.*, 18, pp 361-371

Kropfli, R.A. (1984). Radar probing and measurement of the planetary boundary layer. Part II Scattering from particulates, in Probing the Atmospheric Boundary Layer, ed. D.H. Lenschow, Am. Met. Soc./NCAR, Chapters27a, 27b, pp 183-199

Mayor, S.D., Lenschow, D.H., Schwiesow, R.L., Mann, J., Frush, C.L. and Simon, M.K. (1997). Validation of NCAR 10.6µm CO_2 Doppler lidar radial velocity measurements and comparison with a 915 MHz profiler, *J. Atmos. Ocean. Tech.*, 14, pp 1110-1126

Meischner, P.F., Baumann, R., Holler, H. And Jank, T. (2001). Eddy dissipation rates in thunderstorms estimated by Doppler radar in relation to aircraft in situ measurements, *J. Atmos. Ocean. Tech.*, 18, pp 1609-1627

Palmer, R.D., Bodine, D., Kiemjian, M., Cheong, B., Zhang, G., Cao, Q., Bluestein, B., Ryzhkov, A., Yu, T-Y. and Wang, Y. (2011). Observations of the 10 May 2010 tornado outbreak using OU-PRIME, *Bull. Am. Met. Soc.*, 92, no7, pp 871-891

Pearson G.N. and Collier, C.G. (1999). A compact pulsed coherent CO_2 laser radar for boundary layer meteorology, *Quart J. R .Met. Soc.*, 125, 2703-2721

Pearson, G.N., Roberts, P.J., Eacock, J.R. and Harris, M. (2002). Analysis of the performance of a coherent pulsed fiber lidar for aerosol backscatter applications, *Appl. Opt.*, 41, pp 6442-6450

Pearson, G., Davies, F. and Collier, C. (2009). An analysis of the performance of the UFAM pulsed Doppler lidar for observing the boundary layer, *J. Atmos. Ocean. Tech.*, 26, pp 240-250

Pearson, G., Davies, F. and Collier, C. (2010). Remote sensing of the tropical rain forest boundary layer using pulsed Doppler lidar, *Atmos. Chem. Phys. Discuss.*, 10 , pp 5021-5049

Piper, M. and Lundquist, J.K. (2004). Surface layer turbulence measurements during a frontal passage, *J. Atmos. Sci.*, 61, pp 1768-1780

Post, M.J. and Cupp, R.E. (1990). Optimising a pulsed Doppler lidar, *Appl. Opt.*, 29, pp 4145-4158

Shutts, G. (2005). A kinetic energy backscatter algorithm for use in ensemble prediction systems, *Quart. J. R. Met. Soc.*, 131, pp 3079-3102

Simmons, A. and Hoskins, B.J. (1978). The life cycles of some nonlinear baroclinic waves, *J. Atmos. Sci.*, 35, pp 414-432

Vila-Guerau de Arellano, J., Van den Dries, K. And Pino, D. (2009). On inferring isoprene emission surface flux from atmospheric boundary layer concentration measurements, *Atmos. Chm. Phys.*, 9, pp 3629-3640

Werner, C. (2005). Doppler wind lidar, in *Lidar: Range-Resolved Optical Remote Sensing of the Atmosphere*, ed. C. Weitkamp, Series in Optical Sciences, Vol. 102, Springer, pp 339-342

Wilson, J.W. (1970). Integration of radar and gage data for improved rainfall measurement, *J. Appl. Met.*, 9, pp 489-497

Wilson, J.W. and Miller, L.J. (1972). Atmospheric motion by Doppler radar, in *Remote Sensing of the Atmosphere*, ed. V. E .Derr, Chapters 21a, 27a, 27pp
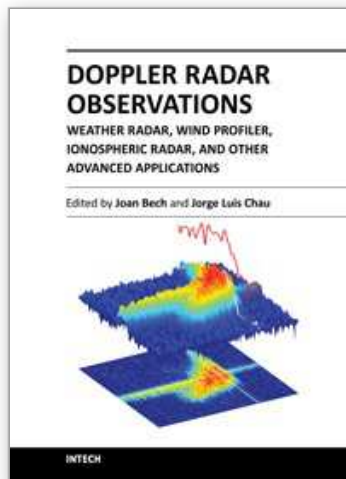
Doppler Radar Observations - Weather Radar, Wind Profiler, Ionospheric Radar, and Other Advanced Applications
Edited by Dr. Joan Bech

Doppler radar systems have been instrumental to improve our understanding and monitoring capabilities of phenomena taking place in the low, middle, and upper atmosphere. Weather radars, wind profilers, and incoherent and coherent scatter radars implementing Doppler techniques are now used routinely both in research and operational applications by scientists and practitioners. This book brings together a collection of eighteen essays by international leading authors devoted to different applications of ground based Doppler radars. Topics covered include, among others, severe weather surveillance, precipitation estimation and nowcasting, wind and turbulence retrievals, ionospheric radar and volcanological applications of Doppler radar. The book is ideally suited for graduate students looking for an introduction to the field or professionals intending to refresh or update their knowledge on Doppler radar applications.

How to reference
In order to correctly reference this scholarly work, feel free to copy and paste the following:

INTECH
open science | open minds